J|A|C|S ARTICLES

Published on Web 05/15/2009

Synthesis, Crystal Structure, and Magnetic Properties of $Bi_3Mn_4O_{12}(NO_3)$ Oxynitrate Comprising $S = 3/2$ Honeycomb Lattice

Olga Smirnova,[†] Masaki Azuma,*[,†] Nobuhiro Kumada,[‡] Yoshihiro Kusano,[§] Masaaki Matsuda,[||] Yuichi Shimakawa,[†] Takahiro Takei,[‡] Yoshinori Yonesaki,[‡] and Nobukazu Kinomura[‡]

Institute for Chemical Research, Kyoto University, Uji, Kyoto 611-0011, Japan, Department of Research Interdisciplinary Graduate School of Medicine and Engineering, University of Yamanashi, Miyamae-Cho 7, Kofu, 400-8511 Japan, Department of Applied Arts and Design, Kurashiki University of Science and the Arts, 2640 Nishinoura, Tsurajima-cho, Kurashiki-shi, Okayama 712-8505, Japan, and Japan Atomic Energy Agency (JAEA), 2-4 Shirakata Shirane, Tokai, Naka, Ibaraki 319-1195, Japan

Received March 12, 2009; E-mail: masaki@scl.kyoto-u.ac.jp

Abstract: Neutron diffraction and FT-IR analysis revealed that the novel oxynitrate $Bi_3Mn_4O_{12}(NO_3)$ (space group $P3$, $a = 4.9692(1)$ Å, $c = 13.1627(3)$ Å) prepared by hydrothermal synthesis is of a new structural type including flat NO_3 layers alternating with blocks of two $PbSb_2O_6$-like layers. Mn^{4+} ($S = {}^3/_2$) forms a regular honeycomb lattice, and magnetic susceptibility data indicated two-dimensional magnetism. Despite its Weiss constant of −257 K, no long-range ordering was observed down to 0.4 K because of the magnetic frustration due to the competition between the nearest and the next-nearest antiferromagnetic interactions.

Introduction

The magnetic properties of a solid reflect the arrangement of the magnetic ions in its crystal structure. Low-dimensional antiferromagnets exhibit a variety of ground states depending on the spin number and the spin configuration,[1,2] and the discovery of new $S = {}^1/_2$ kagome antiferromagnet without lattice distortion[3] and the confirmation of the absence of long-range ordering (LRO) in the $S = {}^1/_2$ triangle antiferromagnet $NiGa_2S_4$[4] have drawn interest to the frustrated two-dimensional magnets. Hydrothermal synthesis can produce crystal structures with cation environments and oxidation states unusual for high-temperature solid-state reaction conditions, and three new allotropic forms of bismuth oxide were prepared under hydrothermal conditions[5−7] because this synthesis method stabilizes the distorted crystal structures due to the $6s^2$ lone pairs of Bi^{3+} and the covalent Bi−O bonds.

A further advantage of hydrothermal reaction is its ability to produce compounds otherwise unstable at high temperatures, such as those containing water or other gas species. $RBi_2O_4NO_3$ (R = Y, Sm, Eu, Gd, Tb, Dy, Er, Yb) obtained by hydrothermal reaction comprises layers built of standing NO_3^- groups, where nitrogen is tetrahedrally coordinated by oxygen.[8] Other bismuth oxynitrates, such as $BiMO_2(NO_3)$ (M = Sr, Ba), have flat NO_3^- groups parallel to the c axis but with bond angles different from 120°.[9] Since NO^{3-} groups separate the M−O networks in these compounds, bismuth oxynitrates with magnetic ions are expected to show two-dimensional magnetism. Planar and regular NO_3^- groups with 120° O−N−O angles are also expected to act as a template for forming magnetic ions into triangular and triangle-derived lattices where magnetic frustration takes place.[2]

In this paper we report the first example of bismuth−manganese oxynitrate $Bi_3Mn_4O_{12}(NO_3)$ prepared by the hydrothermal method, representing a new structural type comprising trigonal NO_3 flat layers alternating with $PbSb_2O_6$-like layers. The bismuth(III) ions occupying three crystallographic sites have distorted octahedral and umbrella-like coordinations, and the edge-sharing MnO_6 octahedra form honeycomb lattices that are well separated by Bi and NO^{3-} layers. Despite the relatively large Weiss constant of −257 K, no long-range antiferromagnetic (AF) ordering was found at temperatures down to 0.4 K because of the magnetic frustration due to the presence of next-nearest AF interaction.

Experimental Section

The sample powder was prepared from $Mn(NO_3)_2 \cdot 9H_2O$ and $NaBiO_3$ (Kanto Chemicals) by hydrothermal reaction−4 days at

[†] Kyoto University.
[‡] Yamanashi University.
[§] Kurashiki University of Science and the Arts.
[||] JAEA.

(1) Johnston, D. C. *Handbook of Magnetic Materials*, vol. *10*; Elsevier: Amsterdam, 1997; p 1.
(2) Ramirez, A. P. *Annu. Rev. Mater. Sci.* **1994**, *24*, 453–480.
(3) Shores, M. P.; Nytko, E. A.; Bartlett, B. M.; Nocera, D. G. *J. Am. Chem. Soc.* **2005**, *127*, 13462–13463.
(4) Nakatsuji, S.; Nambu, Y.; Tonomura, H.; Sakai, O.; Jonas, S.; Broholm, C.; Tsunetsugu, H.; Qiu, Y.; Maeno, Y. *Science* **2005**, *309*, 1697–1700.
(5) Kumada, N.; Kinomura, N.; Woodward, P. M.; Sleight, A. W. *J. Solid State Chem.* **1995**, *116*, 281–285.
(6) Kinomura, N.; Kumada, N. *Mater. Res. Bull.* **1995**, *30*, 129–134.
(7) Kumada, N.; Kinomura, N. *Mater. Res. Soc. Symp. Proc.* **1999**, *547*, 227–232.
(8) Kumada, N.; Takahashi, N.; Kinomura, N.; Sleight, A. W. *J. Solid State Chem.* **1998**, *139*, 321–325.
(9) Ziegler, P.; I.; Grigoraviciute, I.; Gibson, K.; Glaser, J.; Kareiva, A.; Meyer, H. J. *J. Solid State Chem.* **2004**, *177*, 3610–3615.

Table 1. Data Collection and Refinement Details for $Bi_3Mn_4O_{12}(NO_3)$

radiation type	neutron
Formula unit	$Bi_3Mn_4O_{15}N$
Symmetry	Trigonal
Space group	*P*3 (No 143)
Z	1
Lattice parameters:	
a, Å	4.9692(1)
c, Å	13.1627(3)
Instrument	HRPD (JRR-3)
Wavelength	1.82307
Temperature	300 K
Container material	vanadium
2Θ range	12.5−145°
2Θ step	0.05°
Number of reflections	272
Number of variables	42
Profile function	Pseudo-Voight
U	0.29(6)
V	−0.40(11)
W	0.22(4)
Preferred orientation (hkl)	100
Secondary phases	MnO_2 6.7(1) w%
Agreement factors:	
R_p, %	5.68
R_{wp}, %	7.3
R_{Bragg}, %	4.45
R_f, %	2.59
χ^2	2.89
G.o.f.	2.9

533 K—in 70 mL Teflon-lined autoclaves. SEM pictures were taken using a JEOL JSM-6500F, and TEM and ED pictures were taken with a Topcon EM-002B. FT-IR measurements were made with a Jasco FT/IR-4100 apparatus using both ATR reflection mode and KBr transmission mode attachments. TG/DTA measurements accompanied by mass spectrometry results were obtained, in a helium atmosphere at a heating rate 5 K/min in the temperature range from 300 to 1173 K, by using a Rigaku ThemoPlus TG-8120 equipped with a Thermo Mass system. Synchrotron X-ray powder diffraction (SXRD) measurements were made using beamline BL02B2 at the SPring-8 facility. The data were collected with a constant wavelength (λ = 0.422225 Å) at room temperature. Neutron powder diffraction (NPD) measurements were made, using a high-resolution powder diffractometer (HRPD) at the JRR-3 reactor of the JAEA site in Tokai, at a constant wavelength (λ = 1.82307 Å) in a vanadium container at room temperature. EXPO2004[10] and FOX programs[11] were used for crystal structure solution, and the FullProf&Winplotr Suite[12] was used for refinement of the structure. The details of the data collection and of the structure solution and refinement are summarized in Table 1. Magnetic susceptibility was measured with a SQUID magnetometer (Quantum Design MPMS XL) in an external magnetic field of 100 Oe on cooling between 2 and 400 K. The specific heat of a pellet solidified at 6 GPa in a cubic-anvil-type high-pressure apparatus was measured at temperatures between 0.4 and 300 K by a relaxation method with a Quantum Design PPMS.

Results and Discussions

Synthesis and Crystal Structure. The hydrothermal reaction yielded a fine black powder consisting of particles no more than about one micrometer across (Figure 1). X-ray phase analysis revealed only a small amount of MnO_2, and all of the other diffraction peaks seemed to be due to a new phase. TEM studies confirmed the presence of two morphologies: the major phase corresponding to a hexagonal platelet shape and the minor phase corresponding to a needle-like shape (Figure 1). Indexing of the electron diffraction patterns of the major phase provided the approximate dimensions of the hexagonal cell: $a \approx 5$ Å and $c \approx 13$ Å (Figure 2). As no systematic absences were observed, the space group had to be chosen from 16 possible groups. When analyzing the synchrotron X-ray data (not shown) with the lowest hexagonal symmetry group (*P*6), a combination of the direct method of structure solution from powder pattern implemented in EXPO2004 and the direct-space method implemented in FOX allowed us to locate heavy atoms in a structural model similar to $PbSb_2O_6$ (with bismuth in lead sites and with manganese in antimony sites) but having a *c* parameter approximately three times longer. The hexagonal cell includes two $PbSb_2O_6$-like layers separated by a light-atoms layer unsolved from X-ray data. Since the presence of NO_3^- groups in the structure was suggested by FT-IR measurements that showed clear signal with the wavenumber 1380 cm^{-1} (Figure 3), similar to the signal seen in FT-IR spectroscopy results for

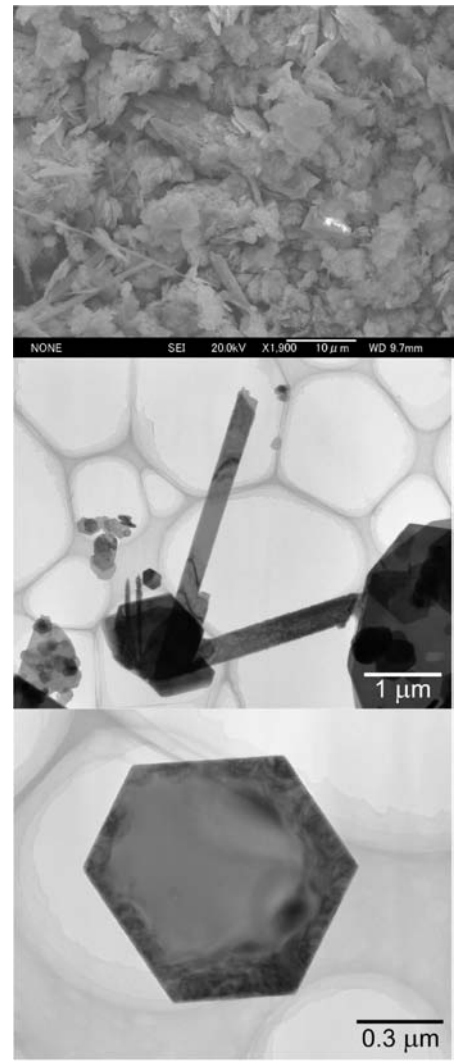

Figure 1. SEM (top) and TEM (middle) photos of the powder obtained by hydrothermal reaction. The bottom TEM image shows a particle of the main phase.

(10) Altomare, A.; Caliandro, R.; Camalli, M.; Cuocci, C.; Giacovazzo, C.; Moliternia, A. G. G.; Rizzia, R. *J. Appl. Crystallogr.* **2004**, *37*, 1025–1028.
(11) Favre-Nicolin, V.; Cerny, R. *J. Appl. Crystallogr.* **2002**, *35*, 734–743.
(12) Rodriguez-Carvajal, J. In Abstracts of the Satellite Meeting on Powder Diffraction of the XV Congress of the IUCr, 1990, 127, Toulouse, France.

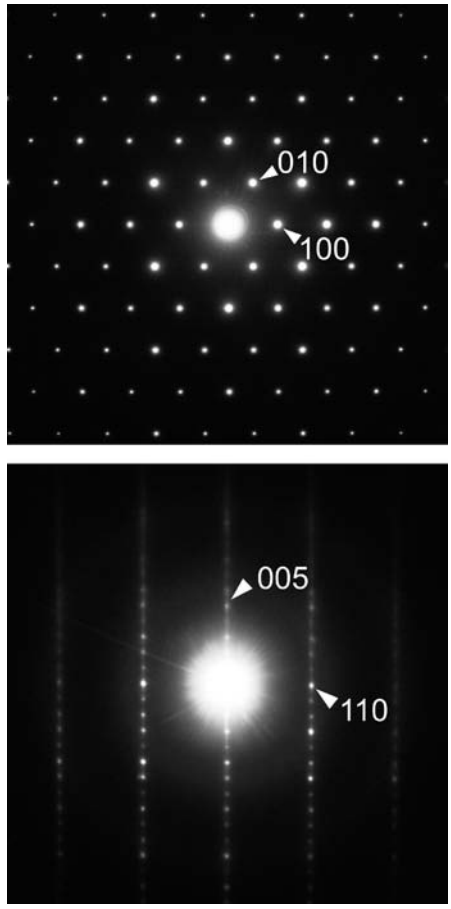

Figure 2. Electronic diffraction patterns of hexagonal $Bi_3Mn_4O_{12}(NO_3)$.

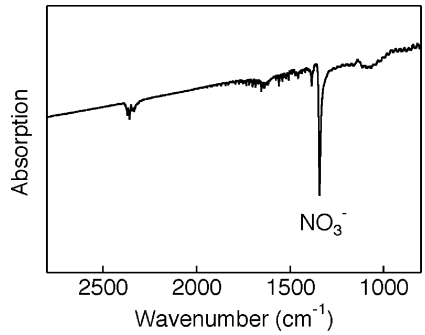

Figure 3. $Bi_3Mn_4O_{12}(NO_3)$ FT-IR spectra measured in the transmission mode.

$YBi_2O_4NO_3$,[8] the neutron diffraction data were analyzed on a model with NO_3^- groups between the two $PbSb_2O_6$-like layers. TG/DTA mass spectroscopy confirmed the presence of nitrogen ions as discussed later. Figure 4 shows the NPD pattern with the result of the Rietveld refinement. Further reduction of the space group to $P3$ was necessary to place the flat NO_3^- group whose presence was indicated by the direct-space analysis of the neutron diffraction data. The absence of inversion symmetry was verified by means of optical second harmonic generation measurement.

The refined crystal structure is illustrated in Figure 5. The structural parameters refined from neutron data are listed in Table 2. Since no sign of off-stoichiometry was observed, the occupancy factors were fixed to unity. The refinement showed the presence of 6.7 wt % MnO_2 as a secondary phase. To our

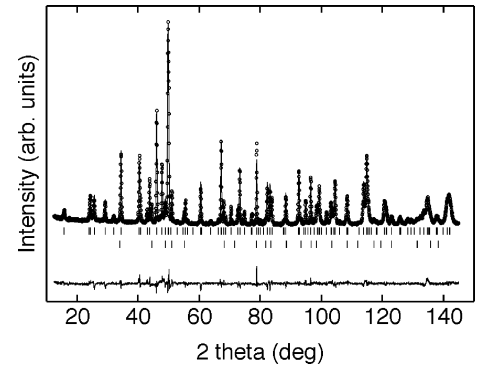

Figure 4. Rietveld plot of neutron data for $Bi_3Mn_4O_{12}(NO_3)$. Observed (circles), calculated (line) and difference (lower line) profiles are shown together with Bragg markers for the $Bi_3Mn_4O_{12}(NO_3)$ phase and MnO_2.

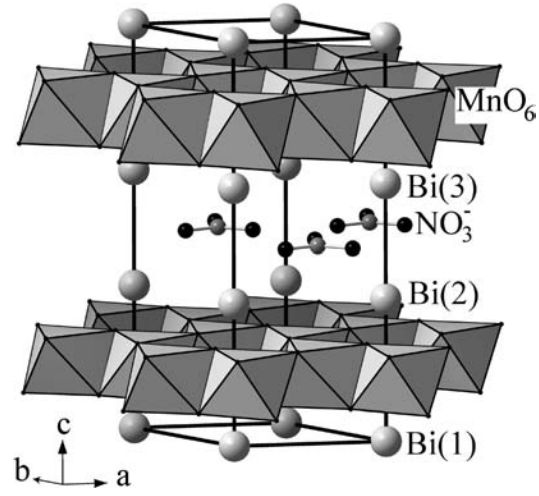

Figure 5. Polyhedral representation of $Bi_3Mn_4O_{12}(NO_3)$ structure.

Table 2. Positional and Thermal Parameters for $Bi_3Mn_4O_{12}(NO_3)$ as Obtained from Neutron Data

atom	Wyck.	fraction	*x*	*y*	*z*	B_{iso} (Å^2)
Bi(1)	1a	1.0	0	0	0.025(4)	0.61(5)
Bi(2)	1a	1.0	0	0	0.673(5)	0.61
Bi(3)	1a	1.0	0	0	0.382(5)	0.61
Mn(1)	1c	1.0	2/3	1/3	0.855(5)	0.35(11)
Mn(2)	1b	1.0	1/3	2/3	0.852(6)	0.35
Mn(3)	1c	1.0	2/3	1/3	0.218(5)	0.35
Mn(4)	1b	1.0	1/3	2/3	0.223(6)	0.35
O(1)	3d	1.0	0	0.381(4)	0.927(5)	0.75(5)
O(2)	3d	1.0	0	0.623(1)	0.762(5)	0.75
O(3)	3d	1.0	0	0.360(4)	0.295(5)	0.75
O(4)	3d	1.0	0	0.626(3)	0.142(5)	0.75
O(5)	3d	1.0	0.475(6)	0.522(6)	0.537(4)	2.56(14)
N	1b	1.0	2/3	1/3	0.535(5)	0.51(16)

knowledge, the novel bismuth manganese oxynitrate represents a new structural type. Selected interatomic distances are listed in Table 3, and the bond valence sums summarized in Table 4 indicate the following valence state: $Bi^{3+}{}_3Mn^{4+}{}_4O^{2-}{}_{12}(NO_3)^-$. The Mn^{4+} oxidation state is consistent with the formation of MnO_2 as the secondary phase. The manganese atoms have octahedral environment, slightly compressed along the *c* axis of the unit cell. The edge-sharing MnO_6 octahedra form honeycomb lattices as schematically illustrated in the inset of Figure 7b. The bismuth atoms, on the other hand, are in distorted environments. Bi1 is also in an octahedron but is shifted from the center. Bi2 and Bi3 have umbrella-like coordinations. They

Table 3. Selected Interatomic Distances for $Bi_3Mn_4O_{12}(NO_3)$

bond	r (Å)	Bond	r (Å)
Bi(1)−O(1) (×3)	2.29(5)	Mn(1)−O(1) (×3)	1.82(5)
Bi(1)−O(4) (×3)	2.41(6)	Mn(1)−O(2) (×3)	2.00(6)
Bi(2)−O(2) (×3)	2.18(5)	Mn(2)−O(1) (×3)	1.84(6)
Bi(2)−O(5) (×3)	3.06(5)	Mn(2)−O(2) (×3)	1.97(6)
Bi(2)−O(5) (×3)	3.08(5)	Mn(3)−O(3) (×3)	1.89(5)
Bi(3)−O(3) (×3)	2.12(5)	Mn(3)−O(4) (×3)	1.86(5)
Bi(3)−O(5) (×3)	3.22(6)	Mn(4)−O(3) (×3)	1.86(5)
Bi(3)−O(5) (×3)	3.23(6)	Mn(4)−O(4) (×3)	1.89(6)
N−O(5) (×3)	1.23(4)		

Table 4. Bond Valence Sums for $Bi_3Mn_4(NO_3)O_{12}$

Bi1	Bi2	Bi3	Mn1	Mn2	Mn3	Mn4	O1	O2	O3	O4
3.0	2.8	3.1	4.1	4.0	4.3	4.3	2.2	1.8	2.4	1.9

have three short Bi2(3)-O2(3) bonds on one side and six long Bi2(3)-O5(5) bonds on the other side. These environmental distortions might be explained by the space needed for the lone pairs of Bi^{3+}. The distance between $PbSb_2O_6$-like layers and NO_3 layers is quite large: the Bi2−O5 distance is 3.1 Å and the Bi3−O5 distance is 3.2 Å. Since each of these distances is significantly greater than the sum of the ionic radii, the bonding should be rather weak.

Thermal Analysis. The existence of nitrogen atoms in the structure was confirmed by the TG measurements accompanied by mass spectroscopy. When the structure is heated in helium it loses NO and O_2 at 723 K and loses more O_2 at 830, 870, and 1050 K (Figure 6). This suggests that $Bi_3Mn_4O_{12}(NO_3)$, like $YBi_2O_4NO_3$,[8] releases the NO_3 group at 723 K, but this suggestion needs to be confirmed by *in situ* XRD study.

Magnetic Properties. Because the $Bi_3Mn_4O_{12}(NO_3)$ pellet solidified at 6 GPa was highly resistive, the system can be regarded as a localized spin system. The temperature dependence of the magnetic susceptibility shown in Figure 7a shows a broad maximum centered at about 70 K. This broad maximum is a characteristic feature of a low-dimensional antiferromagnet and is consistent with the two-dimensional crystal structure. Fitting the data between 300 and 400 K to the Curie−Weiss law $\chi = C/(T-\theta) + \chi_0$ where C is the Curie constant, θ is the Weiss

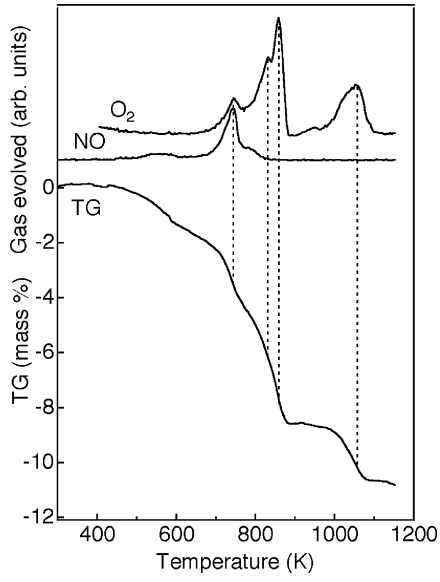

Figure 6. TG and mass spectroscopy data for $Bi_3Mn_4O_{12}(NO_3)$ in helium.

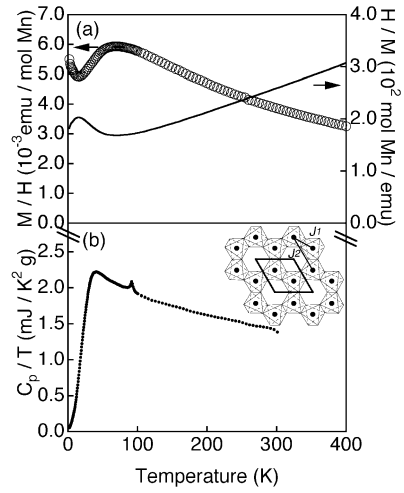

Figure 7. Temperature dependence of the magnetic susceptibility (open circles) and the inverse susceptibility (solid line) (a) of $Bi_3Mn_4O_{12}(NO_3)$. Total specific heat divided by temperature (b) of $Bi_3Mn_4O_{12}(NO_3)$ solidified at 6 GPa. Inset shows the network of Mn spins.

constant, and χ_0 is the temperature-independent term gave $C = 2.21$, $\theta = -257$ K, and $\chi_0 = -1.16 \times 10^{-4}$ emu/mol. This Curie constant is as expected for a Mn^{4+} ($S = {}^3/_2$) system with $g = 2.17$ and is thus consistent with the 4+ oxidation state determined for Mn in the structure analysis. Despite the large AF Weiss constant of −257 K, no sign of LRO was observed. The increased susceptibility seen below 20 K is not an indication of the LRO because no corresponding anomaly is evident in the specific heat data (Figure 7b), and it should be attributed to the presence of an undetected impurity phase or to free spin due to the structural defects. Figure 7b shows the temperature dependence of the specific heat divided by the temperature (C_P/T). Since there is no nonmagnetic reference, the lattice contribution is not subtracted. The small peak at 95 K corresponds to the AF ordering of MnO_2 detected by the SXRD and PND measurements. No other peak is found between 0.4 and 300 K, confirming the absence of the LRO in $Bi_3Mn_4O_{12}(NO_3)$. The C_P/T data show a broad maximum at around 40 K and decrease to zero with decreasing temperature. This suggests the presence of a short-range ordering.

$Bi_3Mn_4O_{12}(NO_3)$ showed a two-dimensional magnetism consistent with the determined crystal structure. Because of its 3-fold symmetry, the honeycomb lattice of Mn^{4+} ($S = {}^3/_2$) is uniform, without any distortion. It should also been pointed out that the orbital ordering as proposed for a $S = 1/2$ Kagome compound $Cu_3V_2O_7(OH)_2 \cdot 2H_2O$[13] does not take place in this compound because of the d^3 nature of Mn^{4+} ion. Despite the AF Weiss temperature of −257 K, no LRO was observed down to 0.4 K. The ground state of an ideal AF honeycomb lattice system with only the AF nearest-neighbor interaction is LRO because the system is free from frustration. If next-nearest interaction is also AF, however, the system is frustrated.[14] In the present compound the nearest AF interaction mediated by the orthogonal Mn−O−Mn bond is rather weak. Considering the Weiss temperature of −257 K and the number of the nearest-neighbor spins, 3, one would expect the exchange interaction to be smaller than 100 K. The next-nearest interaction mediated by the Mn−O−O−Mn bond is therefore not negligible. The

(13) Okamoto, Y.; Yoshida, H.; Hiroi, Z. *J. Phys. Soc. Jpn.* **2009**, *78*, 033701-1–033701-4.
(14) Katsura, S.; Ide, T.; Morita, T. *J. Stat. Phys.* **1986**, *42*, 381–404.

current compound is the first example of frustrated honeycomb antiferromagnet without long-range ordering. The ground states of such systems with classical[14] and quantum[15] spins had been investigated theoretically, but no actual compound had been known. It was predicted that the $S = {}^3/_2$ honeycomb system with $J_2/J_1 > 0.16$ would not exhibit a long-range ordering.[14] Further quantitative analyses of the susceptibility and specific heat data are desirable. It would also be interesting to prepare $Bi_3M_4O_{12}(NO_3)$ with other M cations such as Cr^{4+} ($S = 1$) or V^{4+} ($S = {}^1/_2$) in order to investigate the magnetism of frustrated honeycomb lattices with other spin numbers.

Conclusions

Hydrothermal conditions with nitrate ions stabilize a new type of structure: $Bi_3Mn_4O_{12}(NO_3)$ (space group $P3$, $a = 4.9692(1)$ Å, $c = 13.1627(3)$ Å) containing flat and regular layers of NO_3 composition alternating with blocks of two $PbSb_2O_6$-like layers. The present system is a good model compound of an $S = {}^3/_2$ honeycomb antiferomagnet. Despite the relatively large Weiss constant of -257 K, no AF LRO was found down to 0.4 K because of the magnetic frustration due to the presence of next-nearest AF interaction.

Acknowledgment. We thank Prof. M. Takahashi and Dr. R. Ihara for the SHG measurement and Profs. Y. Motme and M. Greenblatt for the fruitful discussions. This work was supported by the MEXT of Japan Grants-in-Aid for Scientific Research (17105002, 18350097, 19GS0207, 19014010, 19340098, and 19052008), for the Global COE Program, "nternational Center for Integrated Research and Advanced Education in Materials Science, and for Joint Project of Chemical Synthesis Core Research Institute and Elements Science and Technology Project. The synchrotron radiation experiments were performed at the SPring-8 with the approval of the Japan Synchrotron Radiation Research Institute.

JA901922P

(15) Takano, K. *Phys. Rev. B* **2006**, *74*, 140402(R).